Frequency-Domain Equalization for Single-Carrier SFBC Diversity in a Frequency-Selective Fading

Hiroyuki MIYAZAKI† and Fumiyuki ADACHI‡
Dept. of Communications Engineering, Graduate School of Engineering, Tohoku University
6-6-05 Aza-Aoba, Aramaki, Aoba-ku, Sendai, 980-8579 Japan
†miyazaki@mobile.ecei.tohoku.ac.jp, ‡adachi@ecei.tohoku.ac.jp

Abstract— **In a high mobility environment, single-carrier (SC) space-frequency block coding (STBC) diversity achieves better bit error rate (BER) performance than SC space-time block coding (STBC) diversity. However, in a strong frequency-selective fading channel, the BER performance degrades due to the orthogonality distortion of SFBC codeword. In this paper, we propose a frequency-domain equalization (called robust FDE) suitable for SC-SFBC diversity in a frequency-selective fading. The robust FDE weights are jointly optimized based on minimum mean square error (MMSE) criterion taking into account channel variation within a SFBC codeword caused by frequency-selective fading. It is shown by computer simulation that proposed robust FDE always achieves BER performance superior to conventional FDE whose weights are determined without considering the channel frequency variation within a SFBC codeword.**

Keywords-component; Space-frequency block coding, frequency-domain equalization, single-carrier transmission

I. INTRODUCTION

In the next generation wireless communications, broadband data services are demanded even in a high mobility environment. In such an environment, the transmit signal is subjected to a time and frequency doubly selective fading and bit error rate (BER) performance significantly degrades [1]. To overcome frequency-selective fading, single-carrier transmission with frequency-domain equalization (SC-FDE) [2-4] is attractive. SC transmission has lower peak-to-average power ratio (PAPR) property than orthogonal frequency division multiplexing (OFDM) transmission. The use of minimum mean square error (MMSE) based frequency-domain equalization (FDE) takes advantage of channel frequency-selectivity and obtains large frequency diversity gain [2-4].

The use of space-time block coding (STBC) diversity [5-7] in addition to FDE further improves the BER performance. However, in a high mobility environment, the orthogonality of STBC codeword is lost and hence, the BER performance degrades [8]. On the other hand, space-frequency block coding (SFBC) diversity [9-12] can avoid a problem resulting from strong time-selectivity of the channel. However, SFBC diversity can suffer from the frequency-selective fading.

In this paper, we propose a new FDE (called robust FDE) suitable for SC-SFBC diversity in a time and frequency doubly selective channel. The robust FDE weights are jointly optimized based on MMSE criterion taking into account channel variation within a STBC codeword caused by frequency-selective fading while the weights of the conventional FDE [11,12] are determined without considering the channel variation. We evaluate, by computer simulation, the BER performance when using the proposed robust FDE to show that the proposed robust FDE achieves a good BER performance in a time and frequency doubly selective fading channel.

The remainder of this paper is organized as follows. The SC-SFBC diversity is introduced in Sect. II. Sect. III describes the design of the robust FDE. Sect. IV discusses the computer simulation results, and Sect. V offers some conclusions.

II. SC-SFBC DIVERSITY

In this paper, SC-SFBC diversity using $J \times Q$ orthogonal space-time block codes (OSTBC) [7] is considered. It is assumed that the transmitter equips with N_t antennas and the receiver has N_r antennas, respectively. In SC-SFBC diversity using OSTBC, the number J of transmit signal blocks and the number Q of coded signal blocks and the code rate J/Q depend on the number N_t of transmit antennas summarized in Table I [7]. The code rate J/Q of OSTBC decreases from 1.0 when $N_t>2$. On the other hand, an arbitrary number of receive antennas can be available without reducing the code rate J/Q.

TABLE I. RELATIONSHIP BETWEEN N_T, J AND Q.

N_t	J	Q	J/Q
2	2	2	1
3	3	4	3/4
4	3	4	3/4

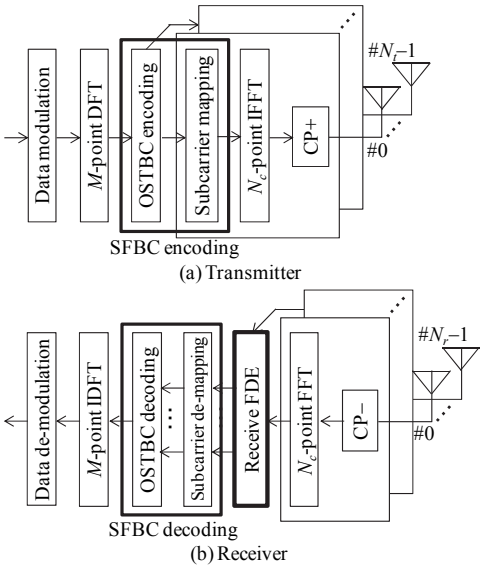

Fig. 1. Transmitter/receiver structures.

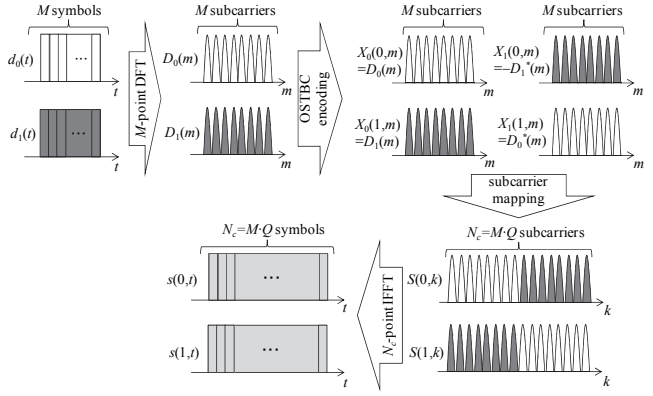

Fig. 2. SFBC and subcarrier mapping (N_t=2).

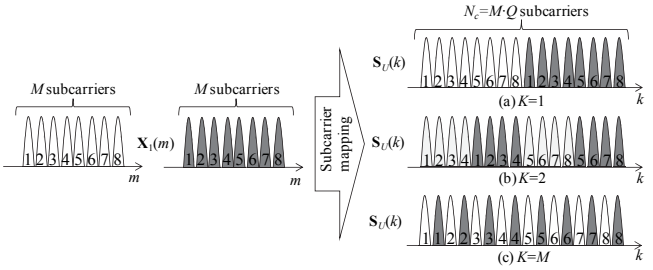

Fig. 3. Subcarrier mapping (N_t=2).

A. Transmitter and receiver srtuctures

Fig. 1 shows the transmitter/receiver structures. At the transmitter, the data modulated signal sequence is divided into J consecutive signal blocks having M modulated symbols each. Each block is decomposed into the frequency-domain signal having M subcarrier components by M-point discrete Fourier transform (DFT). Then, the m-th (m=0,..,M–1) subcarrier components of J consecutive M-symbol blocks are encoded into N_t streams of Q coded subcarrier components. The Q coded signal blocks of M subcarrier components are mapped over an entire bandwidth of N_c=M·Q subcarriers. The coded signal after subcarrier mapping is transformed back to the time-domain signal by N_c-point inverse fast Fourier transform (IFFT). After inserting cyclic prefix (CP), the SC-SFBC signal is transmitted over a time and frequency doubly selective fading channel. At the receiver, after CP removal, the received SC-SFBC signal is transformed into the frequency-domain signal by N_c-point fast Fourier transform (FFT) and then, a series of FDE, subcarrier de-mapping, and OSTBC decoding is performed. The decoded signal is transformed back to the time-domain signal by M-point Inverse DFT (IDFT) for data demodulation.

B. Signal reprensentation

Below, we consider the case of N_t=2 (i.e., J=Q=2).

At the transmitter, the data modulated symbol sequence is divided into a sequence of M-symbol blocks. Each block is decomposed by an M-point DFT into the frequency-domain signal having M subcarrier components. The m-th (m=0,..,M–1) subcarrier components of J=2 consecutive M-symbol blocks are encoded into N_t=2 streams of Q=2 coded subcarrier components. Denoting the frequency-domain transmit signal block as $\{D_j(m);m=0,\ldots,M-1\}$, j=0,…,J–1, the $N_t\times Q$ SFBC coded signal block matrix $(\mathbf{X}_0(m),\ldots,\mathbf{X}_{Q-1}(m))$ with $\mathbf{X}_q(m)=[X_q(0,m),\ldots,X_q(N_t-1,m)]^T$ is expressed as

$$\left(\mathbf{X}_0(m)\quad \mathbf{X}_1(m)\right)=\begin{pmatrix} D_0(m) & -D_1^*(m)\\ D_1(m) & D_0^*(m)\end{pmatrix}\ldots.\ \text{for } N_t=2 \quad (1)$$

Then, the Q=2 coded frequency-domain signal blocks of M subcarrier components are mapped over an entire bandwidth of N_c=2M subcarriers. The coded frequency-domain signal block $\{S(n_t,k):k=0,\ldots,N_c-1\}$, n_t=0,…,N_t–1, after subcarrier mapping can be expressed as $S(n_t,\varepsilon_q(m))=X(n_t,m)$, where $\varepsilon_q(m)$ is the subcarrier mapping index for the mth subcarrier in the qth coded frequency-domain signal block. In this paper, we introduce the number K of spectrum divisions as a parameter in order to discuss the impact of subcarrier mapping to BER and PAPR performances. The subcarrier index, $\varepsilon_q(m)$, is given as

$$\varepsilon_q(m)=(M/K)\left\{Q\left\lfloor\frac{m}{(M/K)}\right\rfloor+q\right\}+(m \bmod (M/K)). \quad (2)$$

Behavior of subcarrier mapping is illustrated in Fig. 3. The coded frequency-domain signal after subcarrier mapping is transformed back to the time-domain signal by N_c-point IFFT. After CP insertion, the SC-SFBC signal is transmitted over a time and frequency doubly selective fading channel.

At the receiver, a super position of N_t transmitted signal is received by N_r antennas. After CP removal, the received signal is transformed into the frequency-domain signal by N_c-point FFT. Denoting the frequency-domain received signal as $\{R(n_r,k);\ k=0,\ldots,N_c\text{-}1\}$, n_r=0,…,N_r–1, the frequency-domain received signal vector $\mathbf{R}(k)=[R(0,k),\ldots.,R(N_r-1,k)]^T$ can be expressed as

$$\mathbf{R}(k)=\sqrt{\frac{2P_t}{N_t\cdot(J/Q)}}\mathbf{H}(k)\mathbf{S}(k)+\mathbf{N}(k), \quad (3)$$

where $\mathbf{S}(k)=[S(0,k),\ldots,S(N_t-1,k)]^T$ is the coded frequency-domain transmit signal vector. $\mathbf{H}(k)=[\mathbf{H}(0,k),\ldots,\mathbf{H}(N_t-1,k)]$ with $\mathbf{H}(n_t,k)=[H(n_t,0,k),\ldots H(n_t,N_r-1,k)]^T$ is the $N_r\times N_t$ channel matrix and $H(n_t,n_r,k)$ is the channel transfer function between the n_tth transmit antenna and the n_rth receive antenna. P_t denotes the transmit power. $\mathbf{N}(k)=[N(0,k),\ldots,N(N_r-1,k)]^T$ is the noise vector and $N(n_r,k)$ is the zero mean complex valued additive white Gaussian noise (AWGN) having variance $2N_0/T_s$ with N_0 and T_s being the single-sided power spectrum density of AWGN and the symbol duration, respectively. Then, the receive FDE is performed. The equalized received signal vector, $\hat{\mathbf{R}}(k)=\left[\hat{R}(0,k),\ldots.,\hat{R}(N_t-1,k)\right]^T$ is given as $\hat{\mathbf{R}}(k)=\mathbf{W}(k)\mathbf{R}(k)$, where $\mathbf{W}(k)=[\mathbf{W}^T(0,k),\ldots,\mathbf{W}^T(N_t-1,k)]^T$ with $\mathbf{W}(n_t,k)=[W(0,n_t,k),\ldots.,W(N_r-1,n_t,k)]$ is the $N_t\times N_r$ receive FDE weight matrix. The received signal after the receive FDE having N_c subcarrier components is decomposed into Q=2 received signal blocks having M subcarrier components each by subcarrier de-mapping. Then, OSFBC decoding is

carried out. The jth decoded received signal $\{\hat{D}_j(m): m=0,\ldots,M-1\}$, $j=0,\ldots,J-1$, is given as

$$\begin{pmatrix}\hat{D}_0(m)\\ \hat{D}_1(m)\end{pmatrix}=\begin{pmatrix}\hat{Y}_0(0,m)+\hat{Y}_1^*(1,m)\\ \hat{Y}_0(1,m)-\hat{Y}_1^*(0,m)\end{pmatrix},\ldots \text{ for } N_t=2 \quad (4)$$

where $\hat{Y}_q(n_t,m)$ is the qth received signal after subcarrier demapping and given as $\hat{Y}_q(n_t,m)=\hat{R}(n_t,\varepsilon_q(m))$. The decoded frequency-domain signal is transformed back to the time-domain signal by M-point IDFT and finally, data demodulation is carried out.

III. Robust FDE for a Strong Frequency-Selective Fading Channel

In this paper, FDE weight is designed so as to minimize mean square error (MSE) between the transmit signal before OSTBC encoding and the received signal before OSTBC decoding. The MSE, e, is given as

$$e=\sum_{j=0}^{J-1}\sum_{k=0}^{M-1}E\left[\left|D_j(m)-\hat{D}_j(m)\Big/\sqrt{\frac{2P_t}{N_t\cdot(J/Q)}}\right|^2\right]. \quad (5)$$

From (1), (3) and (4), (5) can be rewritten as

$$\begin{aligned}e=&\sum_{k=0}^{M-1}\left\{\begin{aligned}&\left|\mathbf{H}(0,\varepsilon_0(m))\mathbf{W}(0,\varepsilon_0(m))+\mathbf{H}^H(1,\varepsilon_1(m))\mathbf{W}^H(1,\varepsilon_1(m))-1\right|^2\\&+\left|\mathbf{H}(1,\varepsilon_0(m))\mathbf{W}(1,\varepsilon_0(m))+\mathbf{H}^H(0,\varepsilon_1(m))\mathbf{W}^H(0,\varepsilon_1(m))-1\right|^2\end{aligned}\right\}\\&+\sum_{k=0}^{M-1}\left\{\begin{aligned}&\left|\mathbf{H}(0,\varepsilon_0(m))\mathbf{W}(1,\varepsilon_0(m))-\mathbf{H}^H(0,\varepsilon_1(m))\mathbf{W}^H(1,\varepsilon_1(m))\right|^2\\&+\left|\mathbf{H}(1,\varepsilon_0(m))\mathbf{W}(0,\varepsilon_0(m))-\mathbf{H}^H(1,\varepsilon_1(m))\mathbf{W}^H(0,\varepsilon_1(m))\right|^2\end{aligned}\right\},\\&+N_t\left(\frac{J}{Q}\right)\left(\frac{P_t}{N}\right)^{-1}\sum_{q=0}^{Q-1}\sum_{n_t=0}^{N_t-1}\sum_{m=0}^{M-1}\left\|\mathbf{W}(n_t,\varepsilon_q(m))\right\|^2\end{aligned} \quad (6)$$

where $N=N_0/T_s$ is the noise power.

A. Conventional FDE

In conventional FDE, the FDE weight is optimized assuming that the channel does not varies within a SFBC codeword (i.e., $\mathbf{H}(n_t,\varepsilon_0(m))\approx\cdots\approx\mathbf{H}(n_t,\varepsilon_{Q-1}(m))$ [11,12]. In this case, the optimization problem is given as

$$\begin{cases}\left\{\begin{matrix}\mathbf{W}(0,\varepsilon_0(m)),\mathbf{W}(1,\varepsilon_0(m))\\,\mathbf{W}(0,\varepsilon_1(m)),\mathbf{W}(1,\varepsilon_1(m))\end{matrix}\right\}=\arg\min e\\ \text{s.t.}\quad \mathbf{H}(n_t,\varepsilon_0(m))=,\ldots,=\mathbf{H}(n_t,\varepsilon_{Q-1}(m))=\overline{\mathbf{H}}(n_t,m)\end{cases}, \quad (7)$$

where $\overline{\mathbf{H}}(n_t,m)=\left\{\sum_{q=0}^{Q-1}\mathbf{H}(n_t,\varepsilon_q(m))\right\}/Q$. By solving $\partial e/\partial\mathbf{W}(0,\varepsilon_0(m))=0,\ldots,\partial e/\partial\mathbf{W}(N_t-1,\varepsilon_{Q-1}(m))=0$, the conventional FDE weight is obtained as

$$\mathbf{W}(n_t,\varepsilon_0(m))=\mathbf{W}(n_t,\varepsilon_1(m))=\frac{\overline{\mathbf{H}}^H(n_t,m)}{\sum_{n_t=0}^{N_t-1}\left\|\mathbf{H}(n_t,m)\right\|^2+N_t\left(\frac{J}{Q}\right)\left(\frac{P_t}{N}\right)^{-1}}. \quad (8)$$

In the conventional FDE, the channel variation in the frequency-domain is not considered. Therefore, in a frequency-selective fading channel, BER performance degrades due to the interference caused by the channel variation.

B. Robust FDE

In this paper, we propose the robust FDE suitable for SC-SFBC diversity in a frequency-selective fading channel. In the proposed robust FDE, multiple FDE weights for a SFBC codeword are jointly optimized taking into account the channel frequency variation within a SFBC codeword (i.e., $\mathbf{H}(\varepsilon_0(m))\neq\cdots\neq\mathbf{H}(\varepsilon_{Q-1}(m))$. The optimization problem for the robust FDE is given as

$$\left\{\begin{matrix}\mathbf{W}(0,\varepsilon_0(m)),\mathbf{W}(1,\varepsilon_0(m))\\,\mathbf{W}(0,\varepsilon_1(m)),\mathbf{W}(1,\varepsilon_1(m))\end{matrix}\right\}=\arg\min e. \quad (9)$$

By solving $\partial e/\partial\mathbf{W}(0,\varepsilon_0(m))=0,\ldots,\partial e/\partial\mathbf{W}(N_t-1,\varepsilon_{Q-1}(m))=0$, the robust FDE weights are obtained as

$$\begin{cases}\mathbf{W}(0,\varepsilon_0(m))=\dfrac{\mathbf{H}^H(0,\varepsilon_0(m))-\mathbf{H}^H(1,\varepsilon_0(m))\left(\widetilde{H}_2(m)/\widetilde{H}_1(m)\right)}{\widetilde{H}_0(m)-\left(\left|\widetilde{H}_2(m)\right|^2/\widetilde{H}_1(m)\right)}\\ \mathbf{W}(1,\varepsilon_0(m))=\dfrac{\mathbf{H}_D^H(1,\varepsilon_0(m))-\mathbf{H}^H(0,\varepsilon_0(m))\left(\widetilde{H}_3(m)/\widetilde{H}_0(m)\right)}{\widetilde{H}_1(m)-\left(\left|\widetilde{H}_3(m)\right|^2/\widetilde{H}_{D,0}(m)\right)}\\ \mathbf{W}(0,\varepsilon_1(m))=\dfrac{\mathbf{H}^H(0,\varepsilon_1(m))-\mathbf{H}^H(1,\varepsilon_1(m))\left(\widetilde{H}_3^*(m)/\widetilde{H}_0(m)\right)}{\widetilde{H}_1(m)-\left(\left|\widetilde{H}_3(m)\right|^2/\widetilde{H}_0(m)\right)}\\ \mathbf{W}(1,\varepsilon_1(m))=\dfrac{\mathbf{H}^H(1,\varepsilon_1(m))-\mathbf{H}^H(0,\varepsilon_1(m))\left(\widetilde{H}_2^*(m)/\widetilde{H}_1(m)\right)}{\widetilde{H}_0(m)-\left(\left|\widetilde{H}_2(m)\right|^2/\widetilde{H}_1(m)\right)}\end{cases}, \quad (10)$$

where

$$\begin{cases}\widetilde{H}_0(m)=\left\|\mathbf{H}(0,\varepsilon_0(m))\right\|^2+\left\|\mathbf{H}(1,\varepsilon_1(m))\right\|^2+N_t\left(\frac{J}{Q}\right)\left(\frac{P_t}{N}\right)^{-1}\\ \widetilde{H}_1(m)=\left\|\mathbf{H}(1,\varepsilon_0(m))\right\|^2+\left\|\mathbf{H}(0,\varepsilon_1(m))\right\|^2+N_t\left(\frac{J}{Q}\right)\left(\frac{P_t}{N}\right)^{-1}\\ \widetilde{H}_2(m)=\mathbf{H}(0,\varepsilon_0(m))\mathbf{H}^H(1,\varepsilon_0(m))-\mathbf{H}(0,\varepsilon_1(m))\mathbf{H}^H(1,\varepsilon_1(m))\\ \widetilde{H}_3(m)=\mathbf{H}(1,\varepsilon_0(m))\mathbf{H}^H(0,\varepsilon_0(m))-\mathbf{H}(1,\varepsilon_1(m))\mathbf{H}^H(0,\varepsilon_1(m))\end{cases}. \quad (11)$$

The second terms in denominator and numerator in (10) contribute to suppress the interference caused by the channel variation in the frequency-domain. In the case of week frequency-selectivity of the channel (i.e., $\mathbf{H}(\varepsilon_0(m))\approx,\ldots,\approx\mathbf{H}(\varepsilon_{Q-1}(m))$), (10) corresponds to conventional FDE weights given as (8).

IV. Computer Simulation

We evaluate, by the computer simulation, the BER performance when using the proposed robust FDE. We consider QPSK data modulation. FFT block size N_c and CP length N_g are set to N_c=128 symbols and N_g=32 samples, respectively. The number N_t of transmit antennas and the number N_r of receive antennas are set to N_t=3 and N_r=2, respectively, as an example. The channel is assumed to be a time and frequency-selective fading. In this paper, we assume perfect CSI can be obtained at the receiver.

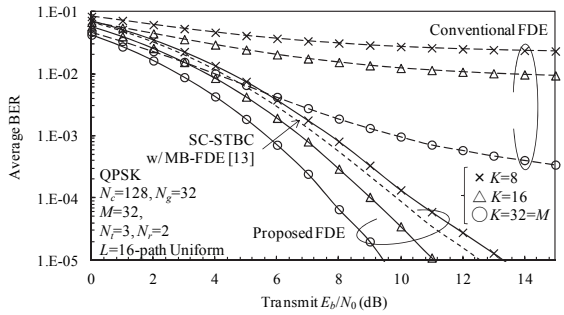

Fig. 4. BER performance.

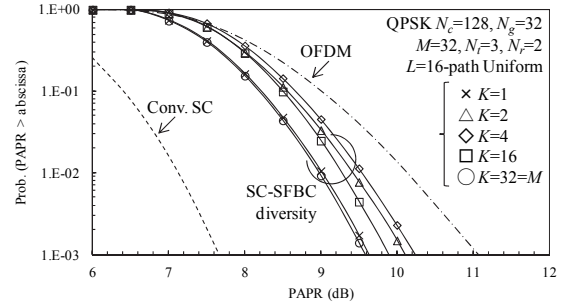

Fig. 5. PAPR performance.

A. BER performance and PAPR performance

Fig. 4 shows the BER performance when using the proposed robust FDE as a function of transmit E_b/N_0. The power delay profile of channel is assumed to be symbol spaced L=16 path uniform power delay profile (the normalized rms delay spread τ_{rms}/T_s=4.61). The normalized maximum Doppler frequency f_DT_B is assumed to be $f_DT_B=1.5\times10^{-1}$, where $T_B=(N_c+N_g)T_s$ is FFT block duration. For the comparison, the performance when using the conventional FDE is also plotted in Fig. 4. It is seen from Fig. 4 that the proposed robust FDE can significantly improve the BER performance compared to the conventional FDE in a frequency-selective fading channel. This is because the proposed robust FDE weights are jointly optimized by taking account into the channel variation in the frequency-domain and hence, it can suppress the interference caused by the orthogonality distortion of SFBC codeword. It is also seen from Fig. 4 that the BER performance improves as the number K of spectrum divisions increases. This is because, as the number K of subcarrier division increases, the distance between subcarriers for a STBC codeword become narrow and as consequence, the channel variation within a SFBC codeword become small (See Fig. 3).

Fig. 5 plots complementary cumulative distribution function (CCDF) of PAPR in SC-SFBC diversity. In this paper, PAPR is calculated as

$$\mathrm{PAPR} = \max\left[\left|s(n_t,t)\right|^2\right] / E\left[\left|s(n_t,t)\right|^2\right], \qquad (12)$$

where $\{s(n_t,t):n_t=0,\ldots,N_t-1,\ t=0,1/8,\ldots,N_c-1\}$ is the 8 times over-sampled transmit signal waveform. For the comparison, PAPRs of conventional SC transmission and OFDM transmission are also plotted in Fig. 5. It is seen from Fig. 5 that PAPR increases as the number of spectrum divisions increases. However, as the number of spectrum divisions further increases, PAPR decreases. The reason for this is explain as follows. When the number of spectrum divisions is relatively small, the phase rotation among subcarriers becomes non-consecutive as the number of subcarrier division increases and as consequence, PAPR increases. However, when the number of spectrum divisions is relatively large, the distance between subcarriers for a common SC signal becomes close to be equal as the number of spectrum divisions increases (See Fig. 3). Therefore, the phase rotation among subcarriers becomes consecutive as the number of spectrum divisions increases and as consequence, PAPR decreases. It is seen from these consideration that the optimal number of spectrum divisions is K=M for both BER and PAPR performances.

It is also seen from Fig. 5 that PAPR of SC-SFBC diversity is higher than that of conventional SC transmission due to SFBC encoding. However, PAPR of SC-SFBC diversity is still lower than that of OFDM transmission. For example, SC-SFBC diversity with K=M can reduce the 0.1% outage PAPR, which is the PAPR value at CCDF=0.1%, by about 1.5 dB compared to OFDM transmission.

B. Impact of time and frequency-selectivity

Fig.6 plots the BER performance when using SFBC diversity with the robust FDE as a function of the normalized maximum Doppler frequency f_DT_B and the normalized rms delay spread τ_{rms}/T_s. The transmit E_b/N_0 is set to 6dB. For comparison, the performances of SFBC diversity with the conventional FDE and STBC diversity with our previously proposed MB-FDE [13] are also plotted in Fig 6. It is seen from Fig. 6 that BER performance of SC-SFBC diversity improves as the normalized rms delay spread increases. However, as the normalized rms delay spread further increases, BER performance of SC-SFBC diversity degrades. The reason for this is explained as follows. In SC transmission, frequency diversity gain increases with increase of the normalized rms delay spread and hence, BER performance improves. However, in SFBC diversity, BER performance degrades as the normalized rms delay spread increases due to the interference caused by the orthogonality distortion of SFBC codeword. Therefore, there exists tradeoff relationship between frequency diversity gain and the interference caused by the orthogonality distortion of SFBC codeword in SC-SFBC diversity. When the normalized rms delay spread is relatively small, the effect of frequency diversity gain is larger than the impact of the interference and therefore, BER performance improves as the normalized rms delay spread increases. On the other hand, when the normalized rms delay spread is relatively large, the impact of the interference is larger than the effect of frequency diversity gain and as consequence, BER performance degrades as the normalized rms delay spread increases. It is seen from Fig. 6 that the robust FDE is more robust against channel frequency-selectivity than the conventional FDE. When f_DT_B=0.01 and the required BER=10^{-3}, the robust FDE can tolerate more than τ_{rms}/T_s=9.2 while the conventional FDE tolerates as small as τ_{rms}/T_s=3.2.

It is also seen from Fig. 6 that SC-SFBC diversity with the robust FDE achieves better BER performance than SC-STBC diversity with MB-FDE when $f_D T_B$>0.03. This is because SFBC diversity can shorten the codeword length compared to STBC diversity. When τ_{rms}/T_s=2.0 and the required BER=10^{-3}, SFBC diversity can tolerate 2 times larger Doppler frequency than STBC diversity.

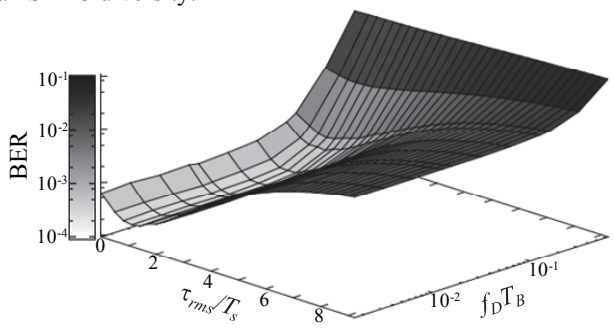

(a) SFBC diversity with the conventional FDE

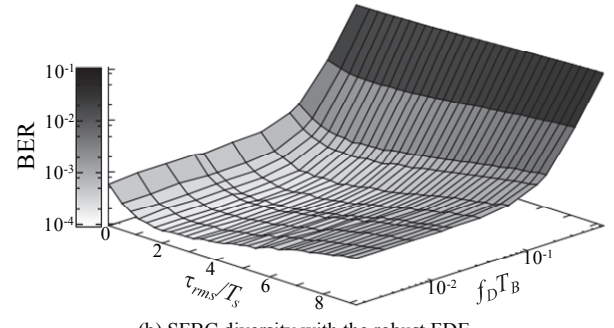

(b) SFBC diversity with the robust FDE

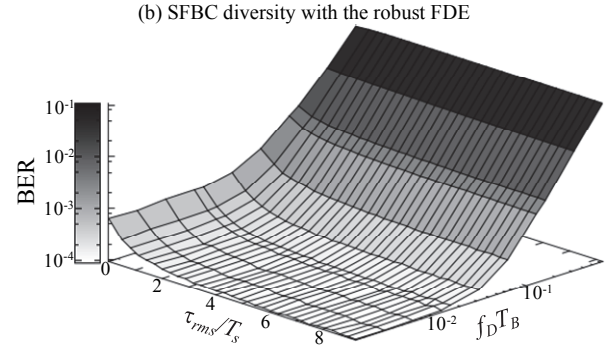

(c) STBC diversity with MB-FDE

Fig. 6. Impact of the normalized maximum Doppler frequency and the normalized rms delay spread.

V. CONCLUSIONS

In this paper, we proposed the robust FDE for SC-SFBC diversity in a frequency-selective fading channel. It was shown by the computer simulation that the proposed robust FDE suppresses the interference caused by the orhtogonality distortion of SFBC codeword and achieves better BER performance than the conventional FDE. Note that the robust FDE performs one-tap FDE only as well as the conventional FDE and therefore, the computational complexity of the robust FDE is almost the same as that of the conventional FDE while achieving better BER performance. Furthermore, the robust FDE can be applied to not only SFBC diversity with receive FDE but also SFBC diversity with transmit FDE. Therefore, by using SFBC diversity with receive robust FDE and SFBC diversity with transmit robust FDE for uplink and downlink transmissions, respectively, both uplink and downlink BER performances can be improved while keeping mobile terminal structure simple as well as our previously proposed SC-STBC time division duplex (TDD) transmission [13-15].

In this paper, we assumed the perfect CSI. The channel estimation suitable for SC-SFBC diversity is left as our future work. Theoretical analysis of SC-SFBC diversity with the robust FDE is also an interesting future study.

REFERENCES

[1] J. G. Proakis and M. Salehi, *Digital communications*, 5th ed., McGraw-Hill, 2008.

[2] H. Sari, G. Karam, and I. Jeanclaude, "Transmission technique for digital terrestrial TV broadcasting," IEEE Commun. Mag., vol. 33, no. 2, pp. 100-109, Feb. 1995.

[3] D. Falconer, S. L. Ariyavistakul, A. Benyamin-Seeyar, and B. Edison, "Frequency domain equalization for single-carrier broadband wireless systems," IEEE Commun.. Mag., vol. 40, no. 4, pp. 58-66, Apr. 2002.

[4] F. Adachi, H. Tomeba, and K. Takeda, "Introduction of frequency-domain signal processing to broadband single-carrier transmission in a wireless cheannel," IEICE Trans. Commun., vol. E92-B, pp. 2789-2808, Sept. 2009.

[5] S. M. Alamouti, "A simple trasnmit diversity technique for wireless communication, " IEEE J. Sel. Areas. Commun., vol. 16, no. 8, pp. 1451-1458, Oct. 1998.

[6] V. Tarokh, H. Jafarkhani, and A. R. Calderbank, "Space-time block coding for wireless communications: performance results," IEEE J. Sel. Areas. Commun., vol. 17, no. 3, pp. 451-460, Mar. 1999.

[7] W. Su, X-. G. Xia and K. J. R. Liu, "A systematic design of high-rate complex orthogonal space-time block codes," IEEE Commun. Letter, vol. 8, no. 6, pp. 380-382, June. 2004.

[8] P. H. Chiang, D. B. Lin and H. J. Li, "Performance analysis of two-branch space-time block coded DS-CDMA systems in time-varying multipath Rayleigh fading channels," IEEE Trans. Vehicular Tech., vol. 56, no. 2, pp. 975-983, Mar. 2007.

[9] J. Yupeng, Y. Dongfeng and W. Dalei, "Performance comparison of STBC and SFBC in turbo coded OFDM systems," Proc. 2005 International Conference on Wireless Communications, Networking and Mobile Computing (WiCOM2005), Wuhan, China, Sept. 2005.

[10] S. Yiu, D. Calin, O. Kaya and Y. Kai, "Distributed STBC-OFDM and distributed SFBC-OFDM for frequency-selective and time-varying channels," Proc. Wireless Communications and Networking Conference (WCNC2012), Paris, France, Apr. 2012.

[11] J. -H. Jang, H. –C. Won and G. –H. Im, "Cyclic prefixed single carrier transmission with SFBC over mnobile wireless channels," IEEE Letters, Signal Processing, vol. 13, no. 5 pp. 261-264, May 2006.

[12] D. –Y. Seol. U. –K. Kwon and G. –H. Im, "Performance of single carrier transmission with cooperative diversity over fast fading channels," IEEE Trans. Commun., vol. 57, no. 9, pp. 2799-2807, Sept. 2009.

[13] H. Miyazaki and F. Adachi, "Robust frequency-domain equalization against doubly selective fading for single-carrier STBC time-division duplex transmission," Proc. the 10th International Wireless Communications and Mobile Computing Conference (IWCMC2014), Nicosia, Cyprus, Aug. 2014.

[14] R. Matsukawa, T. Obara and F. Adachi, "Frequency-domain space-time block coded transmit/receive diversity for single-carrier distributed antenna network," IEICE Communications Express (ComEX), vol. 2, no. 4, pp. 141-147, Apr. 2013.

[15] S. Yoshioka, S. Kumagai, T. Yamamoto, T. Obara, and F. Adachi, "Single-carrier STBC diversity using CDP-CE and linear inter/extra-polation in a doubly selective fading channel," Proc. the 10th IEEE VTS Asia Pacific Wireless Communications Symposium (APWCS2013), Seoul, Korea, Aug. 2013.